Energy Proceedings
Vol 51, 2025
ISSN 2004-2965

Optimizing the gasification characteristics of bio-oil distillation sludge by obtaining co-pyrolysis char with walnut shells#

Yitao Huang[1] ,Xifeng Zhu[1*] ,Chu Wang[2] ,Liang Wang[3]

1 Department of Thermal Science and Energy Engineering, University of Science and Technology of China, Hefei, Anhui 230026, P. R. China

2 School of Energy and Power Engineering, Dalian University of Technology, Dalian, Liaoning 116024, PR China

3 SINTEF Energy Research, P .O. BOX 4761 Torgarden, NO-7465 Trondheim, Norway

(Corresponding Author E-mail: xfzhu@ustc.edu.cn)

ABSTRACT

The presence of bio-oil distillation sludge (DS) disrupts biomass refining and poses health risks. This study investigates DS utilization in industrial bio-oil refining through co-pyrolysis with walnut shell (WS). Char characterization elucidates structural changes induced by co-pyrolysis. Observations show increased DS ratios smoothened the pleated structure of W3D1, with heightened graphitized structure observed at higher DS ratios through Raman analysis. Gasification indices ($R_{0.5}$ and $R_{0.9}$) indicate significant enhancements through co-pyrolysis. Mineral composition analysis revealed silicon in DS reduced ash deposition, while WS blending increased deposition risks due to potassium and calcium content. Investigation into the synergistic relationship between biochar's carbonaceous structure parameters and gasification indices emphasized stronger correlations with $R_{0.9}$, indicating pronounced synergy in later gasification stages.

Keywords: Biomass; Co-pyrolysis char; Carbonaceous Structure; Gasification; Deposition risk

NONMENCLATURE

Abbreviations	
DS(c)	Distillation Sludge (char)
WS(c)	Walnut Shell (char)
WaDb	Char from WS and DS with a:b rate
SEM	Scanning electron microscopy
Symbols	
X	the average conversion rate
R	the gasification index

1. INTRODUCTION

The rapid evolution of the economy, population, and technology has driven a substantial surge in human energy consumption. This surge, in turn, has prompted the widespread depletion of conventional fossil fuels like coal and petroleum. With global primary energy reserves proving inadequate to meet present energy needs, there arises an imperative to explore new energy alternatives to counter the prevailing energy crisis [1]. Amid the sphere of clean energy, biomass energy, especially from environmentally friendly sources, emerges as the most viable contender for fostering substantial development

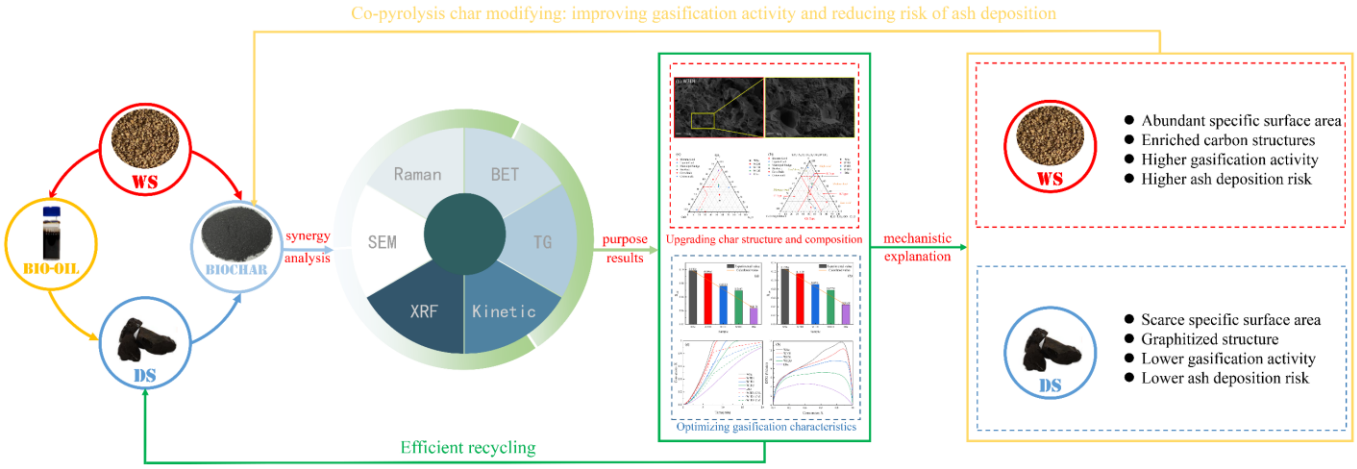

Fig. 1 Graphic abstract

This is a paper for the 16th International Conference on Applied Energy (ICAE2024), Sep. 1-5, 2024, Niigata, Japan.

in renewable energy on a large scale [2]. Biomass energy carries significant advantages over other energy forms due to its widespread availability, expansive distribution, renewable nature, minimal carbon footprint, and low emissions of SO_X and NO_X.

The primary objectives of this study encompass several key facts; (i) acquire carbonaceous structure parameters via scanning electron microscopy, a specific surface area and porosity analyzer, and Raman spectroscopy; (ii) juxtapose gasification indices obtained through thermogravimetric curve to reveal the synergy between WS and DS during co-pyrolysis process; (iii) evaluate the ash deposition risk of the gasification process of pyrolysis char; (iv) quantitatively assess the correlation between the carbonaceous structure parameters and gasification indices of co-pyrolysis char sourced from walnut shell (WS) and distillation sludge (DS). This analysis culminates in establishing a linear relationship between the carbonaceous structural parameters and gasification indices, thereby scrutinizing the pathways for enhancing the gasification of bio-oil distillation residue through the co-pyrolysis carbonization process.

2. MATERIALS AND METHODS

2.1 Raw materials and char preparation

The bio-oil distillation sludge used in the experiment was produced in a bio-oil rectification system independently developed by USTC. The walnut shell was pyrolyzed in a fluidized bed at a reaction temperature of 500°C. The pyrolysis gas is generated in a pyrolysis liquefaction device with the capacity of 500 kg/h. The obtained pyrolysis gas is purified and collected through a cyclone separator and a graded condensation system, and then selected as an aqueous bio-oil in a distillation tower for subsequent distillation experiments. The distillation experiment lasts for 3 hours. After the distillation experiment is completed, the residual solids collected from the bottom of the tower are called bio oil distillation sludge.

WS and DS were mixed in ratios of 3:1, 1:1, and 1:3, thoroughly mixed by mechanical agitation, and sieved through a 60-mesh screen to ensure the uniformity of the mixture. A tube furnace pyrolysis reactor was used for the pyrolysis experiment. In the pyrolysis experiment, a quartz boat containing 4g of sample was placed in the heating area of the pyrolysis reactor. Before the pyrolysis experiment, a high-purity nitrogen gas (99.99%) was purged into the furnace at a flow rate of 200mL/min for 10 minutes, and then the tube furnace was heated from room temperature to 800°C at a heating rate of 10°C/min and maintained for 2 hours to ensure sufficient carbonization. After the pyrolysis experiment, the pyrolysis char was sequentially named WSc, W3D1, W1D1, W1D3, and DSc according to the mixing ratio.

2.2 Gasification test

The isothermal gasification experiment of biomass carbon was performed using a Shimadzu TG-50H thermogravimetric analyzer. Before each isothermal gasification experiment, about 5 mg of prepared biomass carbon was placed in an alumina crucible, and the furnace was purged with high-purity nitrogen (99.99%) for 30 minutes. Then, the temperature was increased from room temperature to 900°C, 950°C, and 1000°C at a heating rate of 20°C/min, respectively. When the temperature in the furnace reached the set temperature, the control program switched the purging gas to CO_2 and conducted the isothermal gasification experiment. When the sample was completely gasified, it can be considered that the isothermal gasification process was completed.

3. RESULTS AND DISCUSSION

3.1 Char characteristic

3.1.1 Char composition and morphology

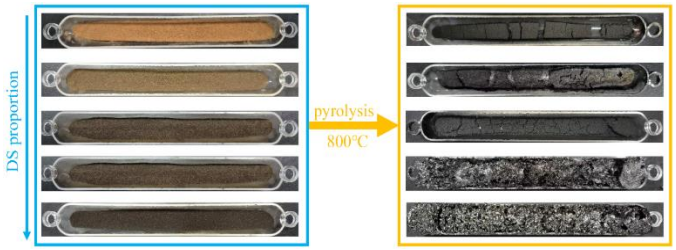

Fig. 2 The morphology of pyrolysis char

The morphology characteristics of pyrolysis char are crucial factors in assessing its suitability as a precursor for gasification. The appearance of experimental samples before and after pyrolysis were depicted in Fig.2. It can be observed that, after pyrolysis process, WSc, W3D1, and W1D1 exhibited varying degrees of volume shrinkage. In contrast, W1D3 and DSc both demonstrated significant expansion phenomena.

The surface structures of the pyrolysis char were observed using scanning electron microscopy (SEM), and the images were presented in Fig.3. It could be seen that the surface of pyrolysis char can be categorized into two types, with WSc and W3D1 having complex surface structures, while the other three types of pyrolysis char have smoother surface morphology. WSc and W3D1 exhibited abundant folded structures on the surface, with hole structures displayed in partly surface. The surface structures of these holes were mainly the result of volatiles escaping from the pyrolysis process. In contrast, the SEM image of DSc revealed a smooth

surface. This was attributed to DS being a solid waste refined from bio-oil distillation, primarily composed of various aromatic compounds and lacking the fibrous structure typical of regular biomass components. The surface of DSc was typically caused by the expansion of polymer aoromatic compounds during pyrolysis, resulting in a smoother surface compared to WSc and W3D1.

Similarly, the SEM images of W1D1 and W1D3 also exhibited surface structures similar to DSc, indicating that, when the blending ratio of DS reached 50%, the morphology of the co-pyrolysis char resembled that of DSc. This may be due to the fact that while WS produced abundant hole structures during pyrolysis by the escape of volatile matter, while DS had a very low volatile matter content and melted during the pyrolysis process, which caused the holes generated during the pyrolysis of WS were filled by liquefied DS during pyrolysis, whereas DS solidified on the surface of WS after the completion of pyrolysis, resulting in a smoother surface morphology of W1D1 and W1D3 compared to that of W3D1. SEM revealed the changes in surface morphology caused by the escape of volatiles and heat deformation during pyrolysis, while the pore structure of pyrolysis char provided further insights into the internal structure of the pyrolysis char after pyrolysis process.

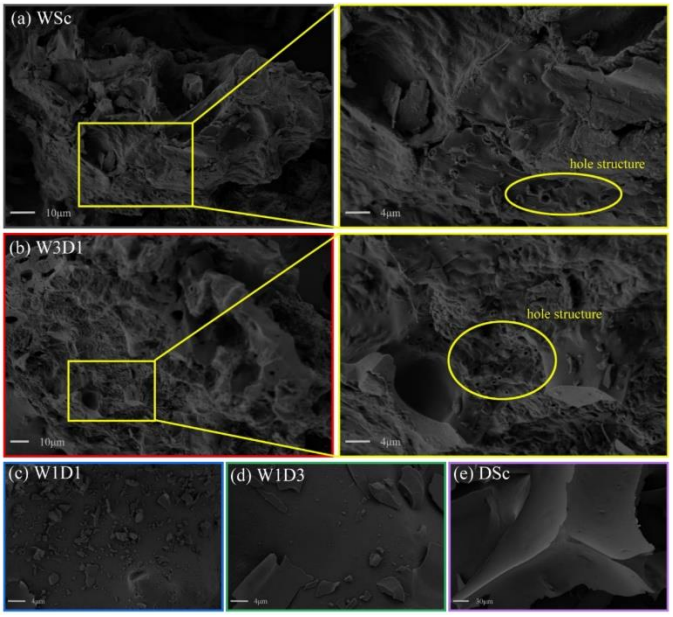

Fig.3 Scanning electron microscopy images of pyrolysis char: (a) WSc, (b) W3D1, (c) W1D1, (d) W1D3, (e) DSc.

3.1.2 Carbonaceous configurations

The microcrystalline structure in biochar can provide reaction sites for gasifying agent molecules to participate in carbon atom reduction reactions, while the regular graphitization structure will significantly hinder the diffusion of gasifying agent molecules inside biochar, thereby inhibiting the progress of gasification reactions. The evolution trends of carbon structures in co-pyrolysis char were characterized using a Raman spectroscopy system, and the resulting Raman spectra are depicted in Fig.4.a. The Raman spectra were further analyzed using five Gaussian peaks, namely D_1 (1350 cm^{-1}), D_2 (1620 cm^{-1}), D_3 (1520 cm^{-1}), D_4 (1245 cm^{-1}), and G (1580 cm^{-1}), for qualitative fitting (Fig.4.b-f) [3]. Herein, The D_1 peak is attributed to the vibration of the carbon microcrystalline edge, the D_2 peak is the shoulder peak of the G peak, mainly caused by the lattice stretching vibration of the graphite structure, the D_3 peak is mainly caused by the amorphous carbon structure in the sample, and the D_4 peak is generated by the C-C and C=C stretching vibration of sp^2-sp^3 bonds or polyene structures. G represents the graphite peak, corresponding to the stretching vibration of aromatic layers in graphite structures, with the peak value characterizing the graphitic carbon structure of the sample.

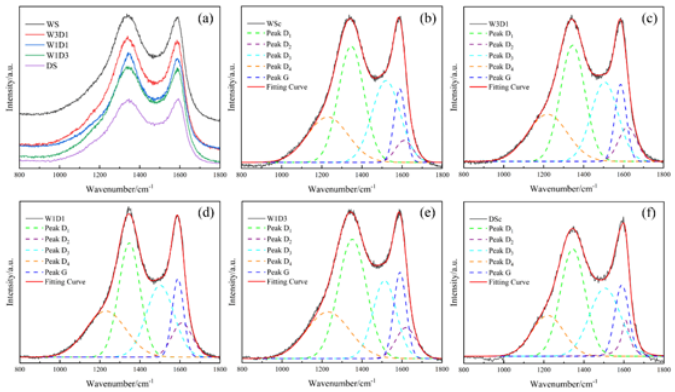

Fig.4 (a) Raman spectra and (b-f) deconvoluted Raman spectra analysis of pyrolysis char.

3.2 Gasification characteristics

3.2.1 Gasification behaviors of co-pyrolysis char

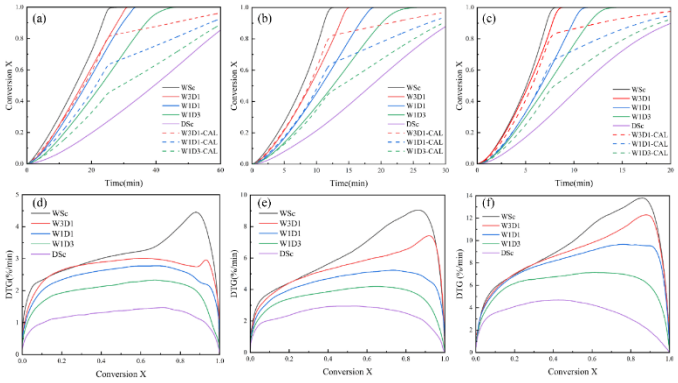

Fig.5 (a) TG and DTG curves of pyrolysis char: (a) TG at 900°C; (b) TG at 950°C; (c) TG at 1000°C; (d) DTG at

900°C; (e) DTG at 950°C; (f) DTG at 1000°C analysis of pyrolysis char.

Fig.5 illustrated the TG and DTG curves of isothermal gasification at 900 °C, 950 °C, 1000 °C. It could be observed that at different gasification temperatures, the gasification rate of WSc was significantly higher than that of DSc. The time required for complete gasification of DS at 900 °C, 950 °C, and 1000 °C was 79.81 min, 46.45 min, and 38.11 min, respectively, indicating that the gasification activity of DSc was extremely low and has a high thermal response temperature. However, the mixing of WS could significantly reduce the time required for the gasification process, the time required for complete gasification of three co-pyrolysis char at 1000°C was shortened to 9.35 min, 12.07 min, and 15.08 min, respectively. The results showed that the gasification rate of co-pyrolysis char increased with the rising blending ratio of WS, consistent with the results from the previous section on carbonaceous structure analysis, where the carbonaceous structure presented in co-pyrolysis char contribute noticeably to their gasification characteristics.

To further investigate the synergistic mechanisms of co-pyrolysis char, this study compared the average conversion rates of calculated data with experimental data, assuming no interaction between the two types of pyrolysis char during gasification. The calculation method for the average conversion rate is as follow:

$$X_{CAL} = a * X_{WS} + (1 - a) * X_{DS} \qquad (Eq.9)$$

The parameter a denotes the blending ratio of WS in the sample. The obtained results are depicted in the scribe lines shown in Fig.6.

Two gasification indices $R_{0.5}$ and $R_{0.9}$ were assessed to characterize the gasification reactivity of the samples during the gasification process, and were compared with the theoretical value of co-pyrolysis char to quantify the synergistic effect between WS and DS during pyrolysis process.

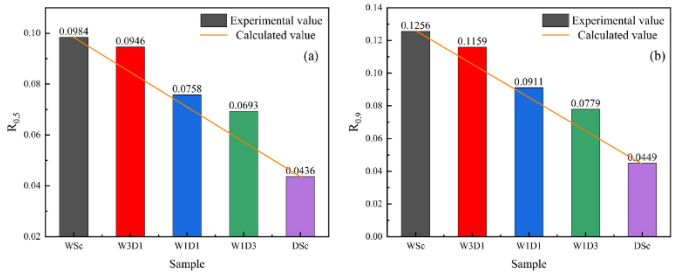

Fig.6 gasification indices (a) $R_{0.5}$ and (b) $R_{0.9}$ of pyrolysis char at 1000 °C

3.3 Ash deposition

3.3.1 Mineral composition

The ash content and slagging behavior of pyrolysis char are crucial factors influencing the recycling of biomass gasification [4]. To gain further insights into the feasibility of co-pyrolysis char in practical biomass energy utilization, the mineral composition and slagging characteristics of pyrolysis char will be discussed in this study, as illustrated in Table 4. Potassium participates in various complex gas-phase reactions at lower temperatures, and elevated potassium content leads to slagging and fouling in the heat transfer zone of the gasifier. The presence of Al_2O_3 raises the melting point of the ash, and higher CaO content contributes to an increase in high-melting-point substances within the ash. In contrast, DSc, as a product of industrial distillation and refining of bio-oil, contains a higher proportion of Fe elements in its ash. These Fe elements arise from the regular wear and tear of industrial equipment during daily cycling operations, and the enriched Fe elements flow with the material into the industrial product, namely, DS. There are notable differences in the mineral composition between WSc and DSc. WSc is rich in alkali metal potassium and alkaline earth metal calcium, while DSc is primarily composed of silicon and iron elements,

Table 1 Mineral composition of pyrolysis char

Sample	CaO	K_2O	SiO_2	P_2O_5	MgO	Al_2O_3	Fe_2O_3	Na_2O	SO_3	Cl_2O	TiO_2
WSc	34.692	28.448	18.972	7.094	3.78	2.712	1.567	0.514	2.086	0.383	0.236
W3D1	28.218	22.721	27.165	6.674	3.516	3.141	3.1478	0.943	3.777	0.404	0.2932
W1D1	19.744	17.151	37.779	5.215	3.067	3.112	4.793	2.096	6.217	0.492	0.334
W1D3	17.841	15.293	39.21	2.886	1.573	2.565	8.784	2.361	8.533	0.579	0.375
DSc	6.962	4.657	55.704	1.853	0.693	2.855	9.986	3.542	12.634	0.682	0.432

with silicon constituting 55.704% and Fe_2O_3 constituting 9.986%.

3.3.2 Deposition risk analysis

SiO_2, CaO, and K_2O are the main components influencing ash fusion in biomass, typically constituting over 50% of the biomass ash content. Therefore, the biomass ash composition is standardized into a SiO_2-CaO-K_2O ternary system to further assess its slagging risk [5]. This system is illustrated in Fig.7a, where some types of coal and biomass were introduced for comparison in this section [6-7]. The right side of the red line in the graph represents the total content of CaO and SiO_2 exceeds 50%, and the K_2O content exceeds 15%. At this point, there is a risk of biomass char ash sintering. Among the five kind of pyrolysis char, only DSc is situated to the left of the red line, indicating a lower risk of sintering during gasification of its ash. The other four co-pyrolysis char exhibit varying degrees of sintering risk. However, from the graph, it can be observed that DSc has a higher SiO_2 content and lower K_2O and CaO content. Therefore, blending with DSc can effectively reduce the sintering risk of co-pyrolysis char, bringing the sample points closer to the red line. This also illustrated that there is a significant difference in ash composition between DSc and ordinary biomass, showing more similarity to coal for DSc.

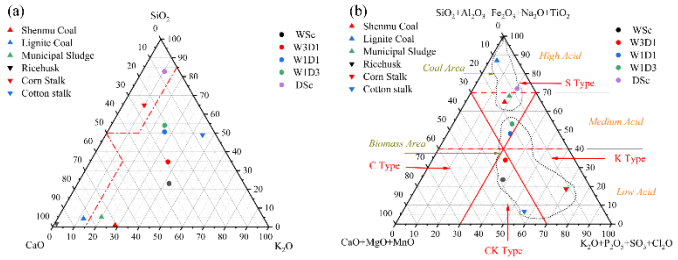

Fig.7 (a) ternary phase diagrams for SiO_2–CaO–K_2O system, (b) $SiO_2 + Al_2O_3 + Fe_2O_3 + Na_2O + TiO_2$–CaO+ MgO + MnO–$K_2O + P_2O_5 + SO_3 + Cl_2O$ system

To explore the influence of other inorganic elements on ash sintering characteristics, a ternary system of SiO_2+Al_2O_3+Fe_2O_3+Na_2O+TiO_2-CaO+MgO-K_2O+P_2O_5+SO_3+Cl_2O (Fig.7b) was further employed to evaluate the ash deposition risk of co-pyrolysis char. Based on the acidity of the ash components, the system is divided by a red solid line into four ash types (S, C, K, and CK) and further classified from top to bottom by red dashed lines into high acid, medium acid, and low acid regions. From the graph, it can be seen that DSc, W1D3, and W1D1 fall into the S type area, where Si, being a high-melting inorganic element, typically results in ash fusion temperatures above 1300°C, indicating a lower risk of ash deposition. However, W1D3 and W1D1 are near the red line, suggesting they have relatively lower ash fusion temperatures, thereby presenting a certain risk of ash deposition. WSc and W3D1 belong to the CK type area, representing Ca and K as the major components of inorganic elements. Their ash fusion temperatures range from 1100°C to 1300°C, resulting in a higher risk of slagging compared to the other three pyrolysis char.

4. CONCLUSIONS

Co-pyrolysis char gasification reactivities increased in the order: DSc < W1D3 < W1D1 < W3D1 < WSc and synergy was found between WS and DS during pyrolysis process, where the gasification time was significantly accelerated from 38.1 min for DSc to 9.35 min for W3D1. Multivariate analysis methods demonstrated that the increasing ratio of WS in improving the carbonaceous structure of DS pyrolysis char while simultaneously curbing its expansion throughout the pyrolysis process.

ACKNOWLEDGEMENT

This work was supported by National Key Research and Development Program of China (52306283). This work was partially carried out at the Instruments Center for Physical Science, University of Science and Technology of China.

REFERENCE

[1] Wang C, Wang RT, Chen T, Zhu XF. Visual experimental study on the effect of heat exchange area on the evolution of biomass pyrolysis vapors in a vertical indirect condensing field. Bioresource Technology. 2022;348.

[2] Hoang AT, Ong HC, Fattah IMR, Chong CT, Cheng CK, Sakthivel R, Ok YS. Progress on the lignocellulosic biomass pyrolysis for biofuel production toward environmental sustainability. Fuel Processing Technology. 2021;223.

[3] Zhou TX, Zhang WW, Luo SY, Zuo ZL, Ren DD. The effect of ash fusion characteristic on the structure characteristics of carbon and the migration of potassium during rice straw high-temperature gasification process. Energy. 2023;284.

[4] He ZM, Deng YJ, Cao JP, Zhao XY. Agglomeration and transformation of different types of inorganic potassium in biomass during co-gasification with coal. Fuel. 2024;357.

[5] HE, Zi-Meng, et al. Agglomeration and transformation of different types of inorganic potassium in biomass during co-gasification with coal. Fuel, 2024, 357: 129728.

[6] YANG, Wei, et al. Mitigation of particulate matter emissions from co-combustion of rice husk with cotton

stalk or cornstalk. Renewable Energy, 2022, 190: 893-902.
[7] Liu H, Wang Y, Xue J, Zhang Y, Yu P, Che D. Experimental study on combustion, ash fusibility and slagging propensity during co-combustion of organic solid waste and lignite. Journal of the Energy Institute. 2023;106.